Journal of Ovonic Research Vol. 10, No. 4, July - August 2014, p. 127 - 139

OPTICAL DISPERSION PARAMETERS OF AMORPHOUS $Se_{70}Te_{30-x}Pb_x$ FILMS

P. KUMAR PAL*, H. GUPTA, L. P. PUROHIT, K. KUMAR, R. KUMAR. R. M. MEHRA[a]
Department of Physics, Gurukula Kangri University, Haridwar-249401, India
[a]School of Engineering & Technology, Sharda University, Greater Noida - 201306, India

The paper reports the optical transmission spectra between 300 to 2000 nm of $Se_{70}Te_{30-x}Pb_x$ (x = 0,2,6,8) films, deposited by thermal vacuum evaporation. The dispersion parameters such as refractive index, extinction coefficient and dielectric constant of the films were computed using transmission data. The refractive index dispersion was analysed in terms of single effective oscillator model and dispersion energy was estimated. The optical bandgap was observed to decrease with Pb contents.

(Received May 2, 2014; Accepted July 25, 2014)

Keyword: Amorphous Materials; Vacuum Deposition; Optical properties

1. Introduction

Over the past decades, an increasing research effort has been devoted in the development of chalcogenide vitreous alloys because a wide variety of present day optical devices strongly rely on their excellent optical dispersion properties. Such as transparency in IR [1] and shift in absorption edge i.e. photo-darkening and photo-bleaching [2, 3]. Chalcogenide vitreous alloys find widespread applications ranging from photovoltaics, IR detectors, optical fibers and waveguides, to photocopiers and medium for optical data storage. $Ge_2Sb_2Te_5$ material is frequently used in rewritable optical data storage and holds considerable promise as a non-volatile phase change memory [4-6]. The optical dispersion parameters of amorphous semiconductors are of great importance because they provide significant structural information, to be used in the design and analysis of various optoelectronic devices [7]. Selenium-Tellurium glasses form one of the most widely studied chalcogenide systems because of their good optical dispersion and extensive glass forming ability [8-15]. In case of Se-Te glasses the bonding nature is divalent, which causes one-dimensional structural stability. Hiroshi Adachi and Kwan C. Kao [8] measured the optical constants of Se-Te films at wavelengths from 0.35 to 2μm using both an ellipsometer and spectrophotometer. They found that increase in the refractive index and the extinction coefficient is linear with Te content in the $Se_{1-x}Te_x$ films. It was attributed to the increase in the density and enhancement in the tailing of localized states in the mobility gap. The addition of an impurity has a pronounced effect on the optical dispersion and structure of amorphous glasses. Thus, a thorough study of optical dispersion was considered important to have a better understanding of the SeTePb system.

In this work, we analyzed the compositional dependence of dispersion parameters such as refractive index, extinction coefficient and dielectric constants of as deposited amorphous $Se_{70}Te_{30-x}Pb_x$ (x =0,2,6,8) films. The dispersion parameters are obtained from the transmittance spectra of the films in the wavelength range 300-2000nm. The addition of Pb in SeTe glasses induced structural modifications exhibited by changes in optical band gap and other optical

* Correspondence author: panchalco@gmail.com

parameters. The data on dispersion of refractive index were analyzed according to the single effective oscillator model proposed by Wemple [16] and Wemple and Didomenico [17].

2. Experiment

2.1 Thin Film Preparation and Structural properties

The stoichiometric composition of $Se_{70}Te_{30-x}Pb_x$ samples in bulk form were prepared by melt-quenching technique. High-purity (99.999%) Se, Te and Pb in appropriate atomic percentage proportions were weighed and put in a cleaned quartz glass ampoules of length 3-4 inches and inner diameter 6 mm. The contents of the ampoule were sealed under a vacuum of 10^{-6} torr and heated at around 800-900K for 15 hours. During the melting process, the ampoules were rocked frequently to intermix the constituents to ensure homogenization of the melt. After giving proper heat treatment, the melt was quenched in ice water to obtain the synthesized material in an amorphous state. The bulk samples were recovered by dissolving the quartz ampoules in HF for 16 hours. Films were prepared by thermal vacuum evaporation (at 10^{-6}torr) of respective bulk glasses onto ultrasonically cleaned corning 7059 glass substrates using HINDHIVAC coating unit (Model No 12A4D). During vacuum deposition, the temperature of the substrates was maintained at 300K to avoid re-evaporation of any condensed component. The thickness of the films was the range of 1 μm.

The structural amorphicity identification of the investigated compositions in the film form was confirmed by X-ray diffraction pattern using a Bruker Advance D8 X-ray diffractometer with monochromatized Cu Kα (=1.54056 Å) radiation. The chemical composition of films was verified by energy dispersive X-ray analysis (EDX).

2.2 Dispersive properties

To determine dispersion parameters and optical band gap of the films as a function of incident light wavelength, the normal incidence optical transmission spectra of as deposited films were taken using a Shimadzu Solidspec 3700 computer interfaced spectrophotometer in the wavelength range of 300-2000 nm. Swanepoel's method [18], based on the interference maxima and minima, appearing in the transmission spectra, was used to calculate dispersion parameters. All the optical dispersion parameters measurements reported in this work were made at room temperature.

3. Results and Discussion

3.1 X-ray Diffraction Pattern

Figure 1 shows the X- ray diffraction patterns for all as deposited films. The absence of characteristic sharp crystalline diffraction peak and presence of humps for $Se_{70}Te_{30-x}Pb_x$ highlight the amorphous nature of the prepared films.

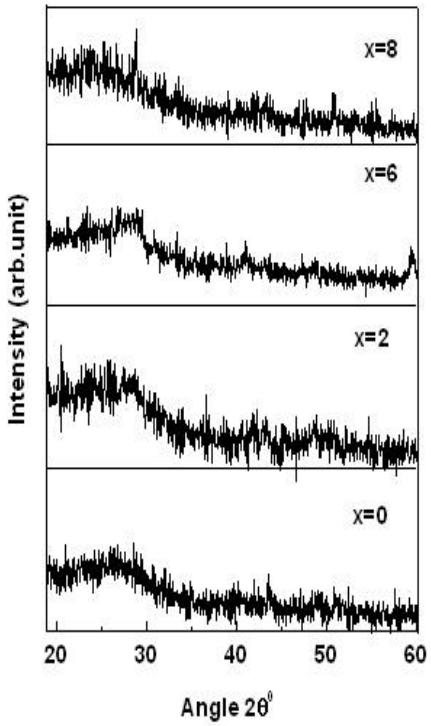

Fig. 1. X-ray Diffraction of as deposited a- $Se_{70}Te_{30-x}Pb_x$(x = 0, 2, 6, 8) films

3.2 Determination of Dispersion parameters

Figure 2 presents the experimental optical transmission of films as a function of incident light wavelength. In the interference free region, red shifts (i.e. photo-darkening) were observed for the films with increasing Pb content. The red shift also depends on the composition/optical bandgap of the films. To determine optical constants, we used Swanepoel's envelope method [18], which is based on extremes of interference fringes and assumes that the films of uniform thickness has a complex refractive index, $n^* = n - ik$, where n is refractive index and k is extinction coefficient which is related to the absorption coefficient α through the relation, $k = \frac{\alpha\lambda}{2\pi}$.

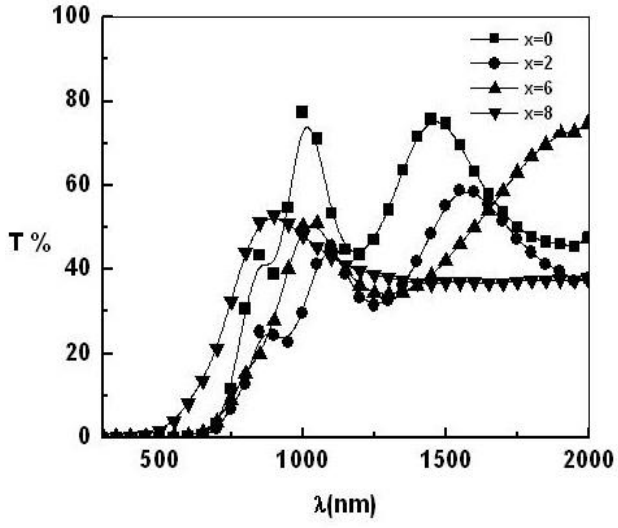

Fig. 2. Transmission spectra of a- $Se_{70}Te_{30-x}Pb_x$ (x = 0, 2, 6, 8) films

The refractive index was calculated from the fringe pattern in the transmission spectra. In the spectral region of weak and medium absorption, where $\alpha \neq 0$, the refractive index n is found to be given by [19],

$$n = \sqrt{N + \sqrt{N^2 - S^2}}\ , \tag{1}$$

where S is the refractive index of corning glass substrate and N is given by

$$N = 2S\left(\frac{T_M - T_m}{T_M T_m}\right) + \frac{S^2 + 1}{2}\ . \tag{2}$$

In this equation, T_M and T_m represent the maximum and subsequent minima in the transmission spectra, respectively. The variation of calculated values of n and k with wavelength for different compositions of a- $Se_{70}Te_{30-x}Pb_x$ are shown in fig.3 and fig.4 respectively. It is observed that refractive index n and extinction coefficient k decreases with increase of wavelength. The values of n and k for different compositions are given in Table 1.

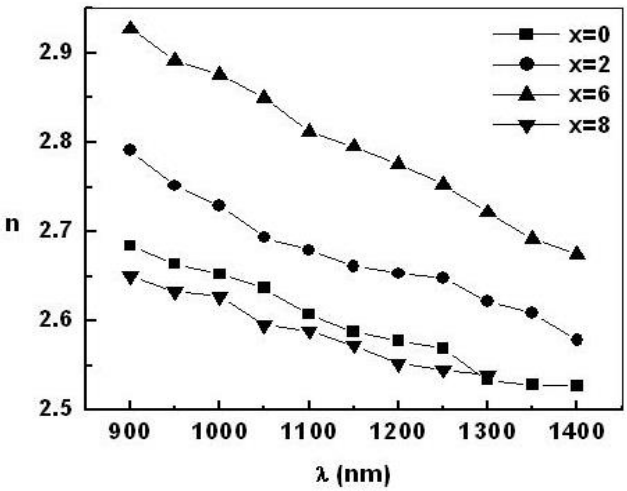

Fig. 3. Dispersion of refractive index for a- $Se_{70}Te_{30-x}Pb_x$ (x = 0, 2, 6, 8) films

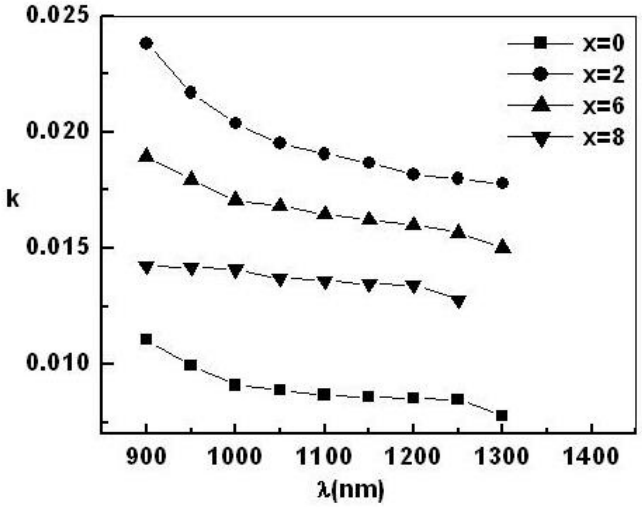

Fig. 4. Dispersion of extinction coefficient for a- $Se_{70}Te_{30-x}Pb_x$ (x = 0, 2, 6, 8) films

The spectral transmittance data was also used to determine the complex dielectric function and dissipation factor of the films. The complex dielectric function describing the linear optical behavior is given as

$$\varepsilon(\nu) = \varepsilon'(\nu) + i\varepsilon''(\nu) = (n + ik)^2 \tag{3}$$

where ε' and ε'' are the real and imaginary parts of the dielectric function, which are related to n and k as [20]

$$\varepsilon' = n^2 - k^2 , \tag{4}$$

$$\varepsilon'' = 2nk \tag{5}$$

and dissipation factor, $\tan\delta$, is expressed as

$$\tan\delta = \frac{\varepsilon''}{\varepsilon'} . \tag{6}$$

The variation of ε',ε'' and $\tan\delta$ with wavelength are shown in figure 5, 6 and 7 respectively.

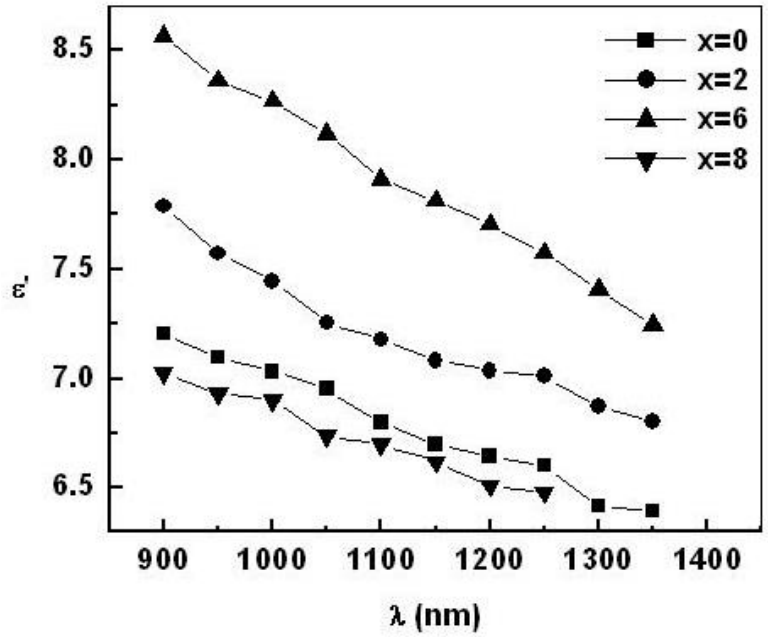

Fig. 5. Dispersion of real part of dielectric constant of a- $Se_{70}Te_{30-x}Pb_x$ (x = 0, 2, 6, 8) films

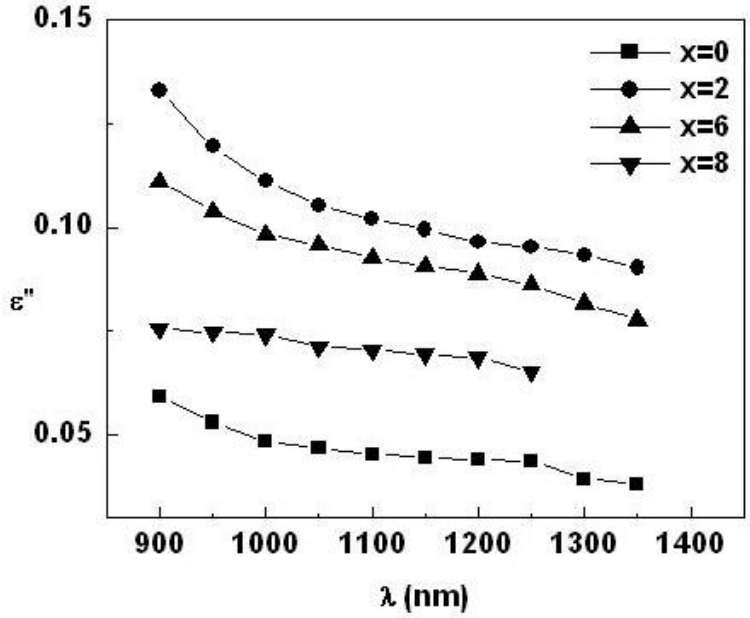

Fig. 6. Dispersion of imaginary part of dielectric constant of a- $Se_{70}Te_{30-x}Pb_x$ (x = 0, 2, 6, 8) films

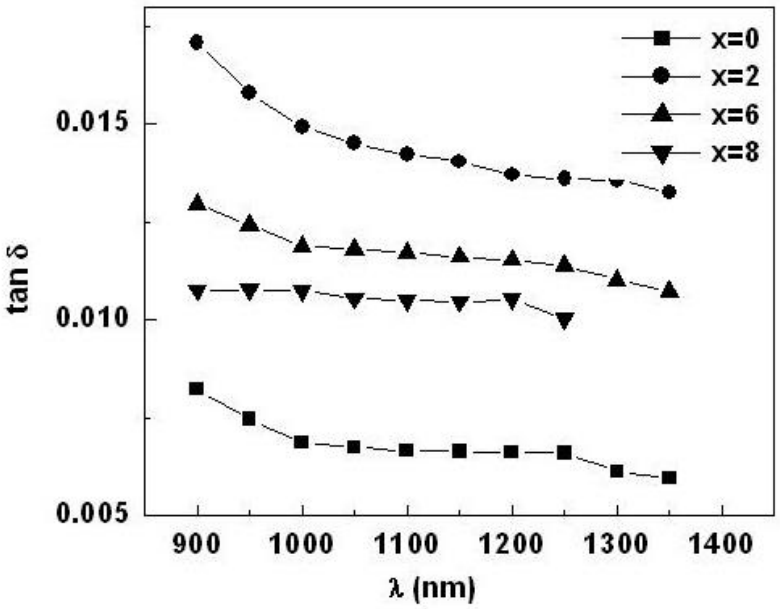

Fig. 7. Dispersion of dissipation factor for a- $Se_{70}Te_{30-x}Pb_x$ (x = 0, 2, 6, 8) films

It was observed from Table 1, that the value of $n>>k$. Therefore, assuming $\varepsilon' = n^2$, the variation of ε' with λ can be examined using the eqn.

$$\varepsilon' = n^2 = \varepsilon_\infty - (\frac{e^2}{\pi c^2}).(\frac{n_c}{m^*})\lambda^2 , \quad (7)$$

where ε_∞ is high frequency dielectric constant, e is the electronic charge, n_c is the carrier density and m^* is the effective mass of the carrier [21]. From a linear re-plot equation, ε' as a function of λ^2, it is possible to estimate ε_∞ and $\frac{n_c}{m^*}$ (figure 8). The values of ε_∞, obtained from the extrapolation of the linear part of the curve, is listed in table 1. The intersection at λ^2 =0 for the linear part of the curve at higher wavelength gives the high frequency dielectric constant. It also observed from the table that ε' and ε_∞ decreases with increase of wavelength. The observed decrease in dielectric constants with wavelength is due to increase in structural disorder.

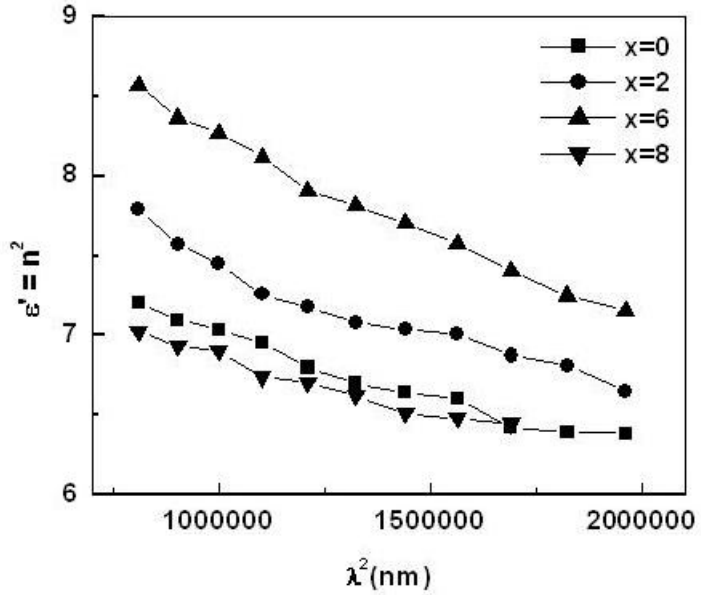

Fig. 8. Plot of relative permittivity versus square of wavelength for a- $Se_{70}Te_{30-x}Pb_x$ (x = 0, 2, 6, 8) films

3.3 Determination of Optical band gap

The absorption coefficient α of amorphous semiconductors generally follows a relation of the form [22]

$$\alpha h\nu = B(h\nu - E_g)^r \quad (8)$$

where ν is the frequency of incident photon, B is a parameter that depends on the transition probability and r is an index which depends on the nature of electronic transition responsible for the optical absorption. Values of r for direct and non-direct transitions are $\frac{1}{2}$ and 2, respectively. The optical bandgap E_g was found by linearly extrapolating the plot of $(\alpha h\nu)^{\frac{1}{r}}$ vs $h\nu$ and finding

the intersection with the abscissa. Figure 9 shows such figures with $r = 2$, exhibiting indirect transitions for amorphous semiconductors. The values of optical band gap E_g are given in table 1 for different compositions. Figure 10 shows the compositional trend of optical band gap for a-$Se_{70}Te_{30-x}Pb_x$ thin films. It was clearly observed that the values of E_g decrease with increase of Pb content. The observed decrease in E_g is related to the decrease in Se-Te bond concentration with the subsequent increase in Pb-Se bond concentration, with lower bond energy.

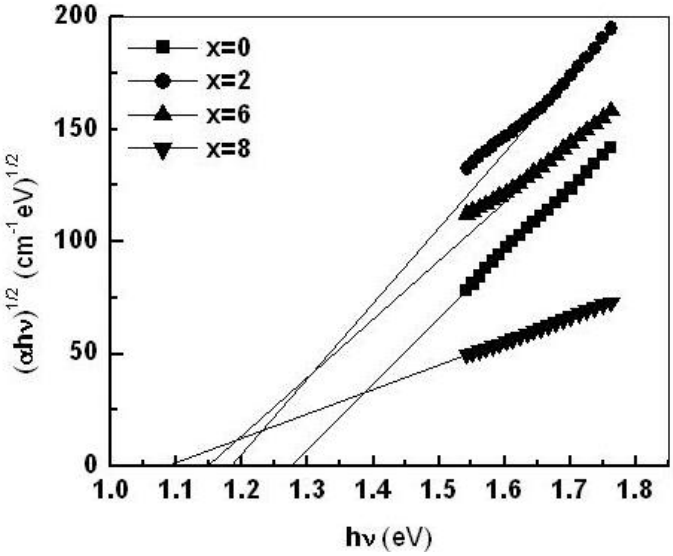

Fig. 9. Plot of $(\alpha h\nu)^{\frac{1}{2}}$ *versus* $(h\nu)$

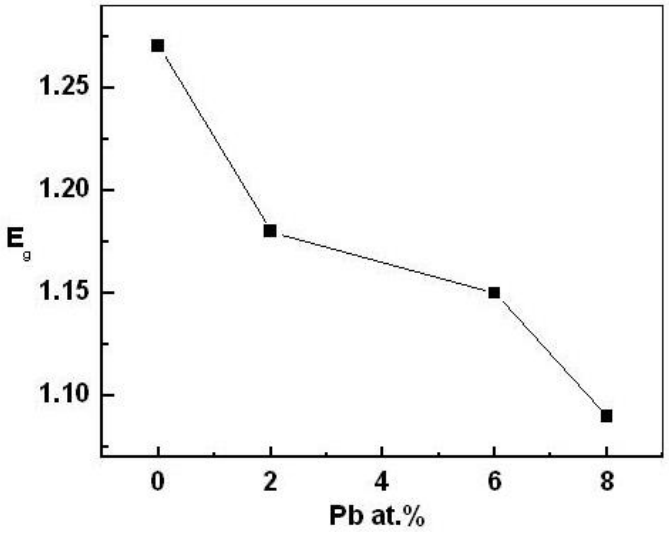

Fig. 10. Plot of optical bandgap versus Pb concentration for a- $Se_{70}Te_{30-x}Pb_x$ *(x = 0, 2, 6, 8) films*

*Table 1. Values of refractive index (**n**), extinction coefficient (**k**), real part of dielectric constant (**ε′**), imaginary part of dielectric constant (**ε″**), dissipation factor (**tan δ**), optical bandgap (**E_g**), and high frequency dielectric constants (**ε_∞**) of a- $Se_{70}Te_{30-x}Pb_x$ (x = 0, 2, 6, 8) films at λ= 900 nm.*

Pb at.%	*n*	*k*	*ε′*	*ε″*	*tan δ*	E_g (eV)	ε_∞
0	2.683	0.0115	7.203	0.0593	0.00824	1.27	7.20378
2	2.790	0.0238	7.789	0.1329	0.01706	1.18	7.78964
6	2.927	0.0189	8.568	0.1110	0.01296	1.15	8.56865
8	2.650	0.0142	7.024	0.0755	0.01076	1.09	7.02504

4. Dispersion analysis of refractive index

The refractive index dispersion behavior was analyzed by the single effective oscillator model proposed by Wemple and Didomenico [16, 17]. They found that the energy dependence of refractive index of amorphous material could be fitted to the dispersion relation, given as

$$n^2(h\nu)-1=\frac{E_d E_0}{E_0^2-E^2}, \tag{9}$$

where $h\nu$ is the photon energy, E_0 is the energy of effective dispersion oscillator (typically near the main peak of the loss part of dielectric function ε_2 spectrum), identified by the mean transition energy from the valance band of the lone pair state to the conduction band state (in these amorphous chalcogenide materials, the valance s state lie far below the top of the valance band and the band edge involves transition between lone pair p states and the anti-bonding conduction band states), and E_d is the so called dispersion energy, which measures the average strength of interband optical transitions. Plots of the refractive index factor $(n^2-1)^{-1}$ against $(h\nu)^2$ allow us to determine the oscillator parameters E_0 and E_d by linear fitting the plots. Such plots are shown in figure 11. The values of dispersion parameters E_0 and E_d, for all the films, as determined from the slope and the intercept on the vertical axis of the figure, are given in Table 2.

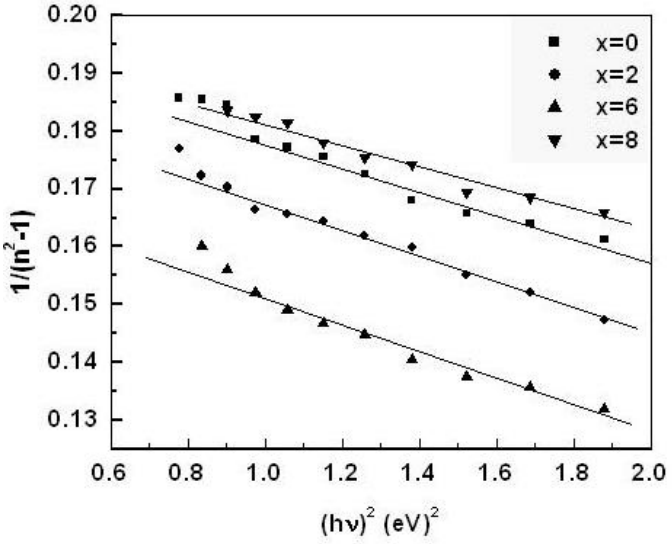

Fig. 11. Plot of refractive index factor $\frac{1}{n^2-1}$ *versus* $(h\nu)^2$ *for a-* $Se_{70}Te_{30-x}Pb_x$ *(x = 0, 2, 6, 8) films.*

Wemple and Didomenico [17] were the first to assign physical significance to the single oscillator parameters. Relating the Kramers-Kronig relation to the real part of the dielectric function, eqn. (10) [23] to eqn. (9), we can have an insight into the physical meaning.

$$\varepsilon_1(h\nu)-1=\frac{2}{\pi}\,p\int_{\nu_t}^{\infty}\frac{\nu'\varepsilon_2(\nu')}{\nu'^2-\nu^2}\,d\nu', \tag{10}$$

where ν_t is the threshold frequency and *p* denotes the principal part.
By identifying $\varepsilon_1(h\nu)$ with the square of refractive index, we can write

$$\frac{E_d E_0}{E_0^2-(h\nu)^2}=\frac{2}{\pi}\,p\int_{\nu_t}^{\infty}\frac{\nu'\varepsilon_2(\nu')}{\nu'^2-\nu^2}\,d\nu'. \tag{11}$$

By expanding both sides of eqn. (11) in powers of ν^2 and equating the coefficients of the different terms, we obtain

$$E_0^2=\frac{M_{-1}}{M_{-3}},\ E_d^2=\frac{M_{-1}^3}{M_{-3}}, \tag{12}$$

where we have introduced the moment M_i of the optical spectrum, which is defined as follows

$$M_i=\frac{2}{\pi}\int_{\nu_t}^{\infty}E^i\varepsilon_2(E)dE\ . \tag{13}$$

As we can see from eqn. (12), E_0 does not depend on the scale of $\varepsilon_2(E)$ (the numerator and denominators are of the same power). In table 2 a decrease was observed in the energy of

effective dispersion oscillator, E_0, for the amorphous $Se_{70}Te_{30-x}Pb_x$ films, with increasing Pb content. The single oscillator energy is considered an average energy gap, and to a good approximation, it varies in proportion to the optical band gap, as was found by Wemple and Didomenico [17] and later by Tanaka [24] because it corresponds to the distance between the centers of gravity of the valance and conduction bands. Therefore, E_0 is related to the average molar bond energy of the different bonds present in the material. Thus, the decrease observed in E_0 for the films belonging to amorphous $Se_{70}Te_{30-x}Pb_x$ films is a consequence of lower bond energy of Pb-Te bonds (250.8 kJ mol^{-1}), when compared with that for the Se-Te (267.52 kJ mol^{-1}). The importance of Wemple and Didomenico model is that it gives very valuable information about the structure of the material through in-depth analysis of the dispersion of refractive index using the values of oscillator strength, E_d. Wemple and Didomenico model relates E_d to other physical parameters of the material through the following empirical relationship [16, 17]:

$$E_d = \beta N_c Z_a N_e \text{ (eV)}, \qquad (14)$$

where $\beta = 0.37 \pm 0.04$ (eV) in covalent materials and $\beta = 0.26 \pm 0.03$ (eV) in ionic materials. N_c is the coordination number of the cation nearest neighbor to the anion, Z_a, is the formal chemical valency of the anion (≈ 2) and, N_e, the total number of valence electrons (cores excluded) per anion. The value of N_e was calculated using the relation:

$$N_e = \frac{6 \times 70 + 6 \times (30 - x) + 4 \times x}{(30 - x) + x}, \qquad (15)$$

Using eqn. (15), $\beta = 0.37 \pm 0.04$, Z_a and values of E_d obtained using eqn. (9), the calculated values of N_c are listed in table 2. In amorphous system, it is reasonable to assume the proportionality between the dispersion energy and the average coordination number. The incorporation of Pb into the structure results in increasing oscillator strength E_d. The increase in E_d with increasing Pb content is primarily a coordination number effect, which characterizes the physical properties of a material. The Pb atoms strongly bond to Te atoms and after Pb-Te bonds are formed, the concentration of Se-Te bonds decrease, which shows an increase in coordination of a- $Se_{70}Te_{30-x}Pb_x$ system.

The values for the static refractive index, *n (0)*, have been calculated from Wemple and Didomenico parameters, E_0 and E_d, by using the eqn. (9) (extrapolated $h\nu \to 0$) as

$$n(0) = \left(1 + \frac{E_d}{E_0}\right)^{\frac{1}{2}}, \qquad (16)$$

The obtained values of *n (0)* are given in table 2. An increase was obtained in a- $Se_{70}Te_{30-x}Pb_x$ films with increasing Pb content.

*Table 2. Values of effective dispersion oscillator energy (E_0), dispersion energy (E_d) dispersion parameters, coordination number of the cation nearest neighbor to the anion (N_c), and static refractive index (**n (0)**) obtained from Wemple and Didomenico model.*

Pb at.%	E_0	E_d	N_c	***n (0)***
0	2.91	14.29	3.218	2.43
2	2.81	14.59	3.249	2.48
6	2.64	14.87	3.212	2.57
8	2.97	17.46	3.621	2.62

5. Conclusion

The dispersion parameters and optical band gap of a- $Se_{70}Te_{30-x}Pb_x$ films have been examined critically. The decrease in the optical band gap with increase in Pb content has been ascertained to the smaller binding energy of Pb-Te bonds than Se-Te bonds. The increase of oscillator strength with increase in Pb content has been attributed to the appearance of highly coordinated (≈ 4) Pb atoms in the host matrix, thereby, increasing overall coordination number.

References

[1] A.Ganjoo, H.Jain, C.Yu, R.Song, J.V.Ryan, J.Irudayaraj, Y.J.Ding, C.G.Pantano, J.Non-Cryst. Solids **352**, 584 (2006).
[2] Y. Utsugi, Phys. Stat. Sol. (b) **212**, R9 (1999).
[3] E.E. Khawaja, C.A.Hogarth, J. Phys. C: Solid-State Phys. **21**, 607 (1988).
[4] M.H.R. Lankhorst, B.W. S. M. Ketelaars, R. A. M. Wolters, Nature Materials **4,** 347 (2005).
[5] T.H. Jenog, M.R. Kim, H.Seo, S. J. Kim, S.Y. Kim, J. Appl. Phys. **86**, 774 (1999).
[6] S. Privitera, E. Rimmi, C. Bongiomo, R. Zonca, A. Pirovano, R. Bez, J. Appl. Phys. **94**, 4409 (2003).
[7] T.Ojima, S.Adachi, J. Appl. Phys. **82**, 3105 (1997).
[8] H. Adachi, K.C. Kao, J. Appl. Phys. **51**, 6326 (1980).
[9] R.M. Mehra, R.Shyam, P.C. Mathur, Phys. Rev. B **19**, 6525 (1979).
[10] R .M. Mehra, G. Kaur, P. C. Mathur, Solid State Communication. **85**, 29 (1993).
[11] R.M. Mehra, Gurinder, A. Ganjoo, R.Singh, P. C. Mathur, Phys. Stat. Sol. (a) **124** k, 51 (1991)
[12] R.M. Mehra, P. C. Mathur, A. K. Kathuria, R.Shyam, Phys. Stat. Sol. (a) **41,** K189 (1977).
[13] J.M.Gonzalez-leal, M.Stuchlik, M.Vlcek, R.Jimenez-Garay, E.Marquez, Appl. Surf. Sci. **246**, 348 (2005).
[14] D. Franta, I.Ohlidal , M. Frumar, J.Jedelsky, Appl. Surf. Sci. **175-176** , 555 (2001).
[15] D. Franta, I. Ohlidal ,M.Frumar,J. Jedelsky, Appl.Surf. Sci. **212-213**,116 (2003).
[16] S. H. Wemple, Phys. Rev. **B 7**, 3767 (1973).
[17] S. H. Wemple, M. Didomenico, Jr., Phys. Rev. B **3**, 1338 (1971).
[18] R. Swanepoel, J. Phys. E: Sci. Instrum. **16**, 1214 (1983).
[19] J. C. Manificer, J. Gasiot, J. P. Fillared, J. Phys. E: Sci. Instrum. **9**, 1002 (1976).
[20] F. Tepehan, N. Ozer, Sol. Energy Mater. Sol. Cells. **30**, 353 (1993).
[21] W. G. Spitzer, H. Y. Fan, Phys. Rev. **106**, 882 (1957).
[22] J. Tauc, Amorphous and Liquid Semiconductors (New York: Plenum press), 171 (1974).
[23] K. Inoue, Katayama, K. Murase, Phys. Rev. B **35**, 7496 (1987).
[24] K. Tanaka, Thin Solid Films **66**, 271 (1980).